SRTTU

JCARME
ISSN: 2228-7922
Journal of Computational and Applied Research in Mechanical Engineering
Vol. 8, No. 2, pp. 199-210
jcarme.sru.ac.ir

Laminar mixing of high-viscous fluids by a novel chaotic mixer

S. M. Hosseinalipour*, P. R. Mashaei, M. E. J. Muslomani

School of Mechanical Engineering, Iran University of Science and Technology, Tehran, Iran

Article info:
Received: 08/07/2016
Accepted: 14/11/2018
Online: 17/11/2018

Keywords:
Chaotic mixer,
Laminar flow,
Average rotational speed,
Mixing index.

Abstract

In this study, an experimental examination of laminar mixing in a novel chaotic mixer was carried out by blob deformation method. The mixer was a circular vessel with two rotational blades which move along two different circular paths with a stepwise motion protocol. The flow visualization was performed by coloration of the free surface of the flow with a material tracer. The effects of significant parameters such as rotational speed of blades, blades length, and rotational speed amplitude on mixing efficiency and time were analyzed by measuring of the area covered by the tracer. The results revealed that increasing rotational speed intensifies stretching and folding phenomena; consequently, better mixing is obtained. Also, a better condition in flow kinematic was provided to blend, as stepwise motion protocol with wider amplitude applied. A reduction in mixing time could be observed while the blades with longer length were used. In addition, it was also found that the promotion of mixing by rotational speed is more effective than that of two other parameters. The quantitative data and qualitative observations proved the potential of the proposed chaotic mixer in the wide range of industrial processes including chemical reaction and food processing in which laminar mixing is required.

1. Introduction

There is no doubt that high-viscous fluids like honey, gel, corn syrup, chocolate, castor oil, glycerol, etc., are involved in different fields such as food and grain processing, chemicals production, pharmaceuticals, petrochemical and refining, polymers, plastics, and paints. On the other hand, the mixing process is necessary to achieve a desirable product in such industries. Regarding the high viscosity of mentioned working fluids, the mixing procedure is laminar. As a result, laminar mixing plays an important role in almost all such industrial areas. Under such condition, turbulent flows are rarely adopted despite their mixing benefits because the large shear stress of high-speed blades in turbulent flow can adversely affect the quality of products. Furthermore, providing turbulent flow for fluids with high viscosity consumes a large amount of energy due to this fact that the motion of blades with high rotational speed in these fluids requires huge power. Chaotic advection is a new approach known to overcome this problem. Aref [1, 2] showed that even laminar mixing can cause an improved mixing while the chaotic behavior of particles is detected. This efficient method has been applied by many

*Corresponding author
email address: alipour@iust.ac.ir

researchers to obtain more homogeneous mixing in laminar flow.

Chein et al. [3] investigated experimentally laminar mixing in several classes of two-dimensional cavity flows by means of material line and blob deformation. Their experimental system comprised of two sets of roller pair connected by a belt which could produce a range of Reynolds number of 0.1-100 and various types of flow field with one or two moving boundaries. They found that the mixing efficiency is a function of the velocity of walls and an optimum value can be found for it. Lemberto et al. [4] conducted several experiments to analyze the mixing performance in a stirring tank under low to moderate Reynolds number conditions. The results demonstrated that the mixing performance can be enhanced under low Reynolds number using a controlled periodic motion of impeller. Yao et al. [5] adopted two unsteady stirring techniques, co-reverse periodic rotation and time-periodic fluctuation of rotational speed, to promote laminar mixing of high viscosity fluids in a stirred tank. The experimental findings proved that the method of co-reverse periodic rotation, only when the Reynolds number is larger than a critical value, can cause significant enhancements in mixing. Moreover, mixing time decreases as the frequency of periodic co-reverse rotation and the amplitude of time-periodic fluctuation increase. Several researchers [6-8] investigated numerically and experimentally the laminar mixing in flow filled between two eccentric cylinders driven periodically. The results revealed that an efficient mixing is achieved when cylinders are periodically rotated with a larger period. Zambaux et al. [9] numerically showed that combining two orthogonal secondary flows can enhance the mixing in an annular configuration using the chaotic advection in flow. Galaktionov et al. [10] studied laminar mixing in a rectangular cavity with a circular cylinder placed in its center and reported that the presence of a rotational cylinder can be a simple method to eliminate the non-chaotic regions. Takahashi and Motoda [11] suggested a novel spatial chaotic mixer by inserting the objects into a vessel agitated by an impeller and stated that their method has a significant influence on mixing efficiency improvement at low Reynolds numbers. Zhang and Chen [12] discussed a new design and implementation of a liquid mixer which could work under different impeller/tank velocity control scheme such as DC signals, periodic signals, and chaotic signals. Comparable experiments showed that the chaotic perturbations injected into the stirred tank can improve the liquid mixing efficiency remarkably. Kato et al. [13] used three non-circle cams to generate the unsteady speed in an impeller revolution and compared mixing performances of this impeller with those of a conventional impeller operated under steady speed. It was demonstrated that the doughnut rings above and below the impeller are disappeared when unsteady mixing is employed because the unsteady motion moves the center of vortexes. Takahashi et al. [14] investigated numerically and experimentally the mixing performance in a vessel agitated by an impeller that inclined itself to promote mixing performance by spatial chaotic mixing. They found that the inclined impeller and eccentric position can reduce mixing time. Hwu [15] proposed a new conceptual apparatus that can be employed to mix high-viscous fluids at low velocities. It consisted of a circular cavity equipped with two blades arranged along the perimeter. The numerical studies showed that the mixing efficiency depends on the length and rotational speed of blades. Mashaei et al. [16] investigated experimentally laminar mixing in a new type of chaotic mixer, proposed by Hwu [15], by means of material line deformation. The flow visualization was carried out by marking of the free surface of the flow with a tracer in working fluid. They demonstrated that the goodness of mixing increases as the rotational speed of blades increases and the mixing performance strongly depends on the length of the rotating blades. Robinson and Cleary [17] evaluated the effect of the impeller on the chaotic mixing in a helical ribbon mixer and reported that an extra ribbon can improve mixing rate over other ribbon geometries. Liu et al. [18] offered a mixer with double rigid-flexible combination impellers. This type of impellers was able to intensify the

motion characteristics of the fluid by suppressing the symmetry structure of the fluid flow. These authors also reported that the mixing efficiency increases with increasing width of the flexible piece.

Shirmohamadi and Tohidi [19] numerically and experimentally investigated a mixer equipped with two rotors with the circular cross-section. The results revealed that the use of blades with sinusoidal motion reduces the weakly mixed regions. Jung et al. [20] suggested a barrier-embedded partitioned pipe mixer (BPPM) and numerically evaluated the mixing process. This mixer was fitted out with orthogonally connected rectangular plate and a couple of barriers. Some methodologies such as the intensity of segregation, interface tracking, and Poincare section were applied to analyze the mixing performance. It was found that BPPM significantly enhances mixing performance as compared with traditional partitioned pipe mixer. Jegatheeswaran et al. [21] used the non-intrusive electrical resistance tomography (ERT) technique to investigate the mixing of non-Newtonian fluids in a chaotic static mixer. The observations proved that Newtonian flow presents an effective axial mixing rather than the non-Newtonian flow.

The objective of this work is to introduce a new design and implementation of a chaotic mixer using blades with stepwise motion. The stepwise motion of blades results in a chaotic advection in the mixer and increases the contacts surfaces of fluid elements based on stretching and folding phenomena. The experimental assessment of mixing is carried out using several tests and the effects of significant parameters such as average rotational speed of blades, blade length, and speed amplitude of blades on mixing efficiency are investigated by means of blob deformation method. The blades of the suggested chaotic mixer are arc-shaped and rotate along circular paths. Consequently, no normal stress imposed on them from the high-viscous fluid. This main feature of the suggested mixer provides a possibility that it is able to operate with low power consumption. It is hoped that the proposed chaotic mixer will be used for the industrial applications such as chemical reaction and food processing in which the rapid mixing of high-viscous fluids is required.

2. Experiments

The liquid mixer is a circular vessel with two blades rotating along a circular path with a stepwise motion. The experimental system is designed to carry out two chief purposes. The first one is to be able to move two blades at various rotational speeds in separate circular paths. The second one is to take pictures of the free surface of flow by means of a digital camera. The experimental apparatus used in this work is shown in Fig. 1. The upper surface of flow is open to atmosphere.

The vessel diameter and height are 0.2m and 0.3m, respectively. The mixer blades are chosen as parts from a pipe with the diameter and height of 0.12m and 0.3m, respectively. This kind of blade is the main innovation of the present mixer. When mixing is caused by pushing fluid, normal share rates and, thus, normal stresses happen in the mixer. Higher viscosity leads to a more considerable value of this type of stress. So, mixers that work based on pushing fluids are subjected to a remarkable resistance force and torque, resulting in consuming a large amount of energy. In the present study, the arc-shaped blades move in a circular path and mixing is usually generated by shear stress and the normal stress is negligible; consequently, less amount of energy is required. The distance between the center of the circular path, where the blade is rotated along, and the vessel is 0.03m, and the gap between the blades and the bottom of the vessel is set 0.005m. The schematic diagram of the experimental apparatus and sketch of a top view of the circular tank are shown in Fig. 2(a) and (b), respectively. The experiments are carried out by the blades with various lengths ($L = \frac{\pi}{6}R_b, \frac{\pi}{3}R_b$ and $\frac{\pi}{2}R_b$) and two similar step motors are used in order to rotate the blades.

The required signals to drive motors are generated utilizing two identical drivers. The input signal to drivers is supplied using a microcontroller ATMega32 which is programmed by a code written in Bascom.

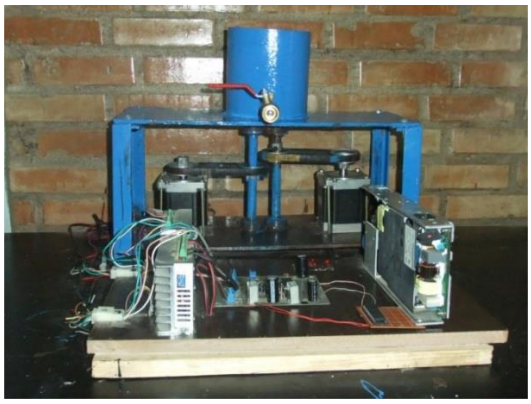

Fig. 1. Experimental set-up.

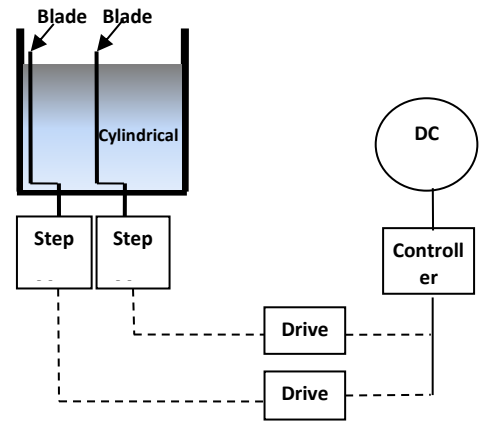

(a)

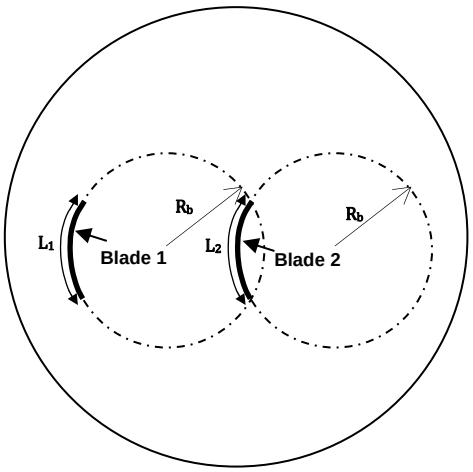

(b)

Fig. 2. (a) Schematic diagram of experimental apparatus and (b) sketch of the top view of rotational blades.

The computer code is changeable with respect to average rotational speed, length and rotational speed amplitude of blades in each experiment. The working fluid is glycerin which fills the vessel to a height of 0.29m (0.01m less than vessel height). In order to analyze mixing performance, deformation of material blob, which is made up of a polymeric dye, is photographed through the top of mixer with a Fuji camera F770EXR every 9 s. The value of diffusion coefficient of dye into working fluid is quite small (about 10-8cm^2/s). So the effect of diffusion on the spreading of the dye in glycerin is approximately negligible [3]. Moreover, as the density of tracer (dye) is less than glycerin, it is reasonable that the effect of buoyancy to be considered negligible. This fact is seen at the end of experiments when a layer of dye is observed on the fluid surface. Another important point is to seek in this study is the ability to create a two-dimensional flow. To achieve this purpose, the polymeric dye, as material blob of tracer, is injected nearly 2–3 mm below the upper surface by a thick needle syringe, as suggested by Niederkorn and Ottino [22]. Each photo is analyzed using a combination of a computer and processor code. The blades are rotated with a discontinuous motion which is defined as the stepwise motion, as introduced by Hosseinalipour et al. [23]. This motion protocol is indicated by the wave form in Fig.3. It is understandable from this figure that the blades change their rotational speed from maximum to minimum and vice versa in every 60 degrees of rotation. Furthermore, it can be seen that when one blade rotates with a maximum value of rotational speed the other one is set to rotate with the minimum value. Another point related to the motion of blades is that while a blade rotates clockwise another does this counterclockwise.

2.1. Mathematical equations and explanations

In order to explain the physical behavior of flow in the chaotic mixer, governing equation of laminar flow should be considered as follow [24]:

$$\frac{\partial \boldsymbol{u}}{\partial t} + (\boldsymbol{u}.\nabla)\boldsymbol{u} = -\frac{1}{\rho}\nabla p + \upsilon\nabla^2\boldsymbol{u} \quad (1)$$

in which $\boldsymbol{u}$, t, p, ρ and υ are velocity vector, time, pressure, density, and kinematic viscosity, respectively.

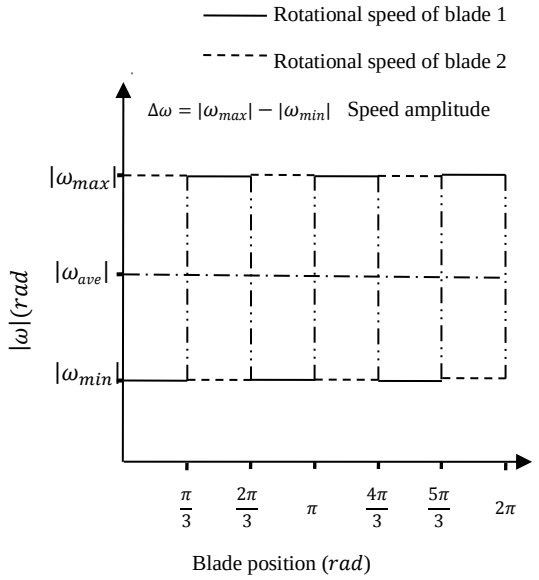

Fig. 3. Rotational speed protocol of two blades in a revolution.

Based on scale analysis and dimension variables, Eq. (1) can be presented as [24]:

$$\frac{\partial \boldsymbol{u}^*}{\partial t^*} + (\boldsymbol{u}^*.\nabla^*)\boldsymbol{u}^* = -\nabla^* p^* + \frac{1}{Re}\nabla^{*2}\boldsymbol{u}^* \quad (2)$$

where superscript "*" refers to the dimensionless form of variable, as extensively discussed in [24], and Re is Reynolds number based on vessel diameter for flow in this geometry which is defined as:

$$Re = \frac{\rho R_b \omega_{ave} D_v}{\mu} \quad (3)$$

in which R_b,ω_{ave}, D_v and μ are the density, blade radius, average rotational speed of blades, vessel diameter and dynamic viscosity, respectively. As the vessel area is physically dominant and the thickness of the blade is negligible, the vessel diameter is considered as the characteristic length. Next point related to Reynolds number is physical properties of the working fluid. Although the mixing process includes two different fluids, the amount of primary fluid (glycerin) is more than 99%; thus, physical properties of glycerin are considered in calculating Reynolds number.

It is clear that the Reynolds number is low for high viscous fluid and; thus, the effect of the diffusion term become stronger. In other words, advection phenomenon cannot play a significant role in laminar mixing because of reduced Reynolds number, as can be inferred from Eq. (2). Consequently, a type of kinematic of flow is required to intensify the stretching and folding of fluid elements, leading more contact surfaces, meaning a better diffusion and mixing.

3. Data reduction

There are several possible parameters which can affect the mixing performance in the proposed mixer. The controlling parameters of are: (1) the average rotational speed of blades, (2) the length of blades, (3) the rotational speed amplitude of blades, (4) the initial position of blades, (5) the radius of blades, and (6) the distance between the centers of vessel and circular paths of blades. Taking into account the high-time-consuming and expensive nature of studying all the above-mentioned factors, the current research focuses on the average rotational speed, rotational speed amplitude, and the length of blades. In addition, the initial position of blobs is considered approximately identical so that the same experimental condition provided in all experiments. For the working fluid under consideration, average rotational speeds of 7.5, 15 and 30rpm (0.39, 0.78 and 1.56 1/s) are applied for blades, which correspond to Reynolds numbers of about of 5, 10 and 20, respectively. In order to qualitatively evaluate the mixing, the free surface of working fluid is photographed at various durations (t= 0, 9, 36, 63, and 99 s). The produced images can show the structure of dye during the mixing process. To have a better and convenient comparison, a Matlab code is developed to change the real images to black-white images. This is carried out by assigning black and white colors to surface covered by dye and surface void of dye, respectively. A typical photo of the actual image and its corresponding processed image are

shown in Figs. 4 (a) and (b), respectively. In order to analyze the mixing performance quantitatively, mixing index (*MI*) is defined as the ratio of the number of colored pixels to the number of total pixels (Eq. (2)), as discussed in the previous works of the authors [23-25].

$$MI = \frac{Number\ of\ colored\ pixeles}{Number\ of\ total\ pixeles} \times 100\ \% \quad (4)$$

(a)

(b)

Fig. 4. Typical photo of (a) the actual one and (b) the processed one ($L = \frac{\pi}{3} R_b$, ω_{ave} =15 ($Re \simeq 10$), t=36s).

Higher *MI* represents more colored surface and therefore the tracer distribution increases as *MI* increases. Another important parameter that evaluates the mixing performance at the end of the experiment is average mixing index, MI_{ave}, which is defined as:

$$MI_{ave} = \frac{\int MI dt}{T}\ \% \quad (5)$$

where T is overall time of experiment.

In order to qualitatively discuss mixing performance in this section, as suggested by Swanson and Ottino [6], the regular regions are the empty spaces of dye and the chaotic region is the region over where dye spreads. In addition, the mixing time refers to the required time to reach a homogeneous state. Under this situation, the *MI* profiles become approximately constant.

4. Results and discussion

4.1. Effect of rotational speed on mixing

As the average rotational speeds of blades have an important effect on flow and, thus, on the mixing performance, preliminary experiments are carried out to analyze the deformation of the material blob in the vessel at various average rotational speeds, as shown in Fig. 5(a-c). In these experiments, the length of both blades is chosen as $L = \frac{\pi}{6} R_b$. The deformation of material blob for $\omega_{ave} = 7.5$ rpm is illustrated in Fig. 5(a). It is clearly seen from this figure that the material blobs slowly move in the vessel and only are stretched until t=9 s. But, as the mixing time increases, the material blob can be folded and more pieces of material lines are generated, therefore, more areas of free space are covered by tracer, as illustrated in Fig. 5(a) at t= 36 s.

With a comparison between processed photographs related to t=36, 63 and 99 s in Fig. 5(a), it is found that the free surface of mixing is so gradually covered by tracer as the blades are rotated with $\omega_{ave} = 7.5$ rpm, resulting in increasing mixing time. For this case, the free surface of fluid is not completely covered by tracer as the experiment time is finished. Fig. 5(b) shows the deformation of the material blob at various times for $\omega_{ave} = 15$ rpm. One can see that the material blob can be folded and stretched even before t=9 s. Although the regular region is yet seen at t=36 s in Fig. 5(b), its size decreases compared with the experiment related to $\omega_{ave} = 7.5$ rpm (see Fig. 5(a)). According to Fig. 5(b), the tracer distributes over the free surface quickly and, thus, mixing time decreases dramatically as it is compared with Fig. 5(a), especially in the initial times of experiment. The processed photographs of blobs deformation for $\omega_{ave} = 30$ rpm at various times are shown in Fig. 5(c). It is obviously seen from this figure that the two blobs cover the free surface of flow quickly, and the regular regions decrease in less time in comparison with two previous tests (see

Fig. 5(a) and (b). This is due to the fact that the stretching and folding phenomena and, thus, the chaotic regions become more remarkable with increasing average rotational speed of blades.

The mixing index profiles as a function of the time for various average rotational speeds of blades equal to 7.5, 15 and 30 rpm are depicted in Fig. 6. According to this figure, the *MI* increases as the rotational speed and time increase and the best value of about 90% is found for $\omega_{ave} = 30$ rpm at the end of the experiment (i.e. t=99 s). That is, when the rotational speed is low, the mixing time is more than the whole experiment time (i.e. 99 s).

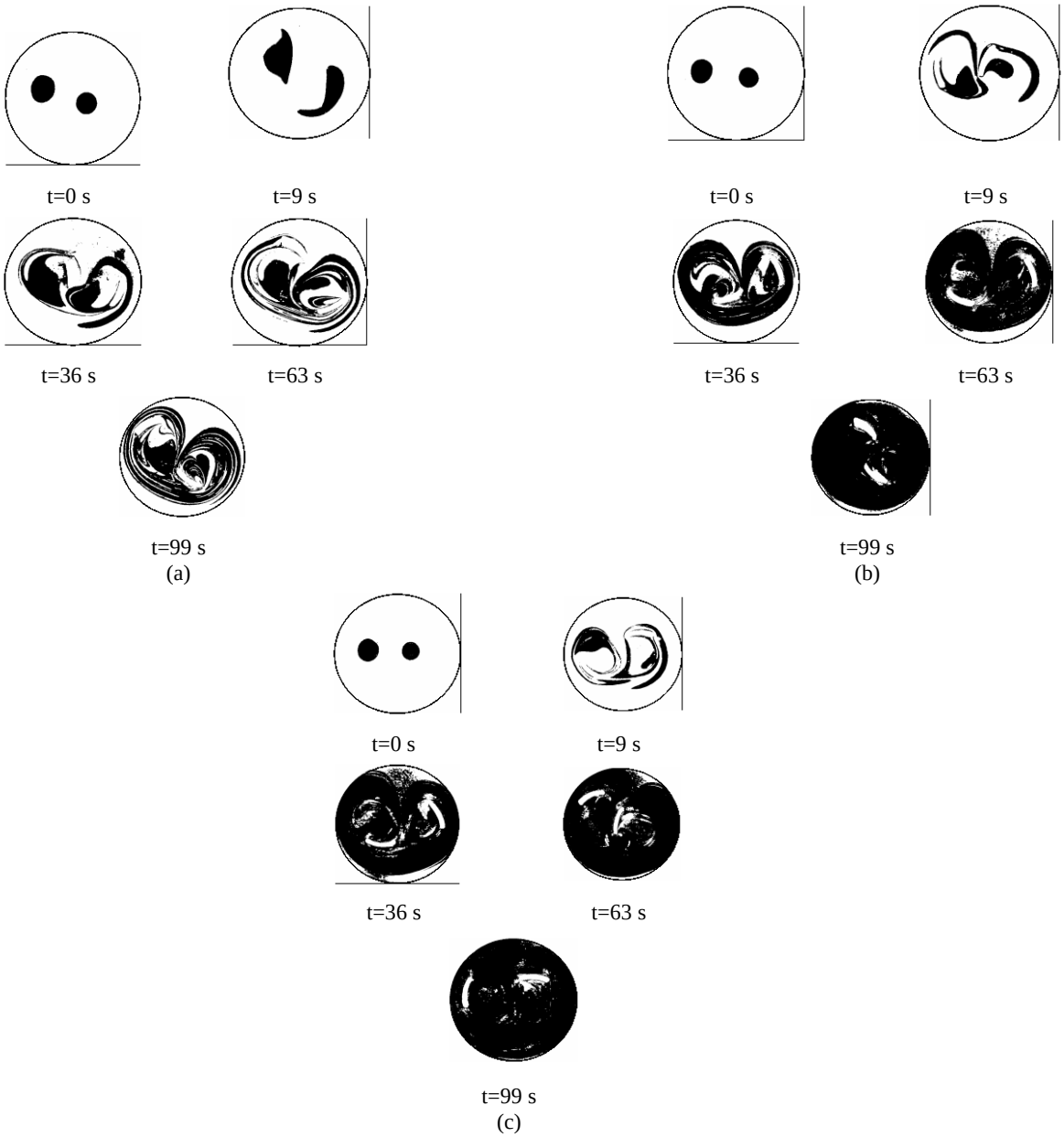

Fig. 5. Deformation of blob at various average rotational speed; (a) $\omega_{ave} = 7.5\text{rpm}(Re \simeq 5)$(Re), (b) $\omega_{ave} = 15\ rpm(Re \simeq 10)$, and (c) $\omega_{ave} = 30\ rpm(Re \simeq 20)$ ($L = \frac{\pi}{3}R_b$ and $\Delta\omega = 10\ rpm$ for all cases).

The average mixing index for $\omega_{ave} = 7.5$, 15 and 30 rpm are 27.6%, 56.6% and 68%, respectively. Based on these results, the mixing at $\omega_{ave} = 15$ is about 105% better than that of at $\omega_{ave} = 7.5$, whereas the average mixing index of $\omega_{ave} = 30$ is only 20% greater than that of $\omega_{ave} = 15$. This implies that although the increase in rotational speed significantly improves mixing performance, the increasing trend of the average mixing index decreases as average rotational speed increases. Such behavior of average mixing index can be explained as follows:

As the rotational speed increases, the amount of regular regions decreases more and more because of intensifying successive stretching and folding phenomena occurring for fluid elements in the mixer, and therefore less non-chaotic areas remain to destroy by increasing rotational speed, consequently, the effect of rotational speed decreases. The phenomena, which is a direct result of chaotic advection, can be considered the most useful features of the present mixer. Because a good mixing can be obtained as blades rotate with a relatively low speed, and consequently, a lower amount of energy is required to turn them.

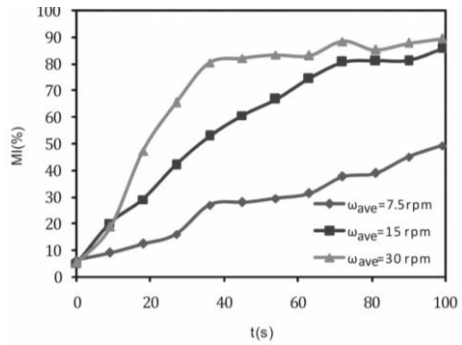

Fig. 6. Effect of average rotational speed on mixing index ($L = \frac{\pi}{3}R_b$ and $\Delta\omega = 10$ rpm for all cases).

4.2. Effect of blade length on mixing

As it is also interesting to analyze the influence of blade length on the deformation of material blobs, the structure of material blob for various lengths of blades at different times of experiment is depicted as demonstrated in Fig. 7(a–c). According to these figures, the increase in the length of blades leads to a reduction in regular and segregated regions, causing relatively better mixing. For example, with a comparison of processed photograph between $L = \frac{\pi}{6}R_b$ and $L = \frac{\pi}{2}R_b$cases at t=36 s, it is observed that the more colored surface, and thus mixing performance can be obtained for $L = \frac{\pi}{2}R_b$ case. However, the mixing of patterns related to various lengths of blades become similar after about 80 s, as one can perceive in photos related to t=99 s in Fig. 7(a–c).

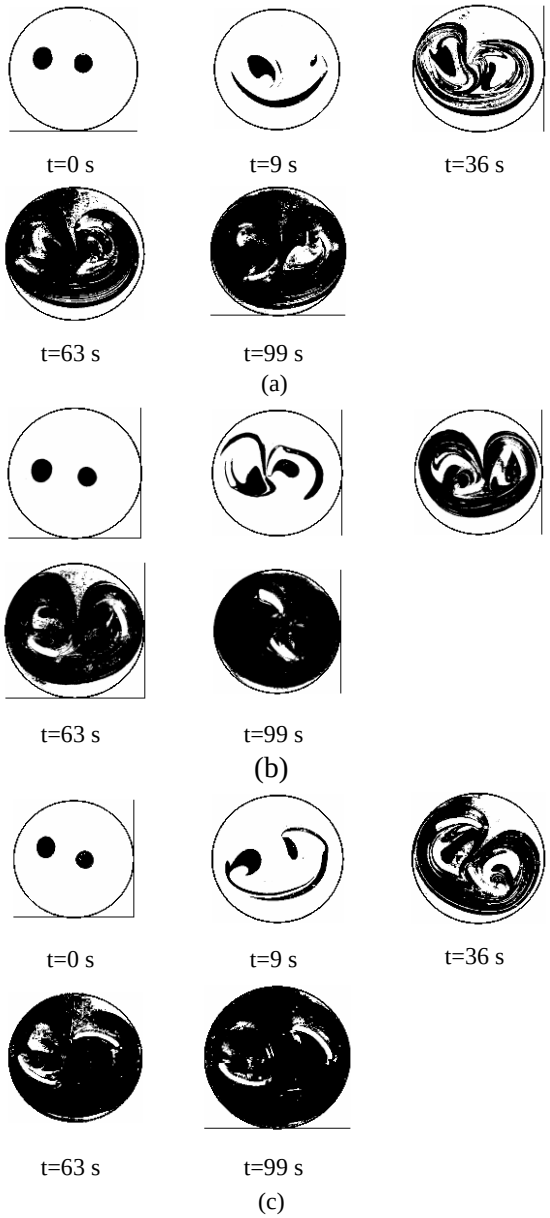

Fig. 7. Deformation of blob for various values of the length of blades; (a) $L = \frac{\pi}{6}R_b$, (b) $L = \frac{\pi}{3}R_b$, (c) $L = \frac{\pi}{2}R_b$ ($\omega_{ave} = 15\ rpm (Re \simeq 20)$ and $\Delta\omega = 10\ rpm$ for all cases).

Fig. 8 depicts the variations of *MI* as a function of time for various considered blades at $\omega_{ave} = 15$ rpm. The figure shows that increasing blade length decreases the mixing time. The blades with the lengths of $L = \frac{\pi}{6}R_b$, $L = \frac{\pi}{3}R_b$ and $L = \frac{\pi}{2}R_b$ have mixing times approximately 90 s, 72 s and 54 s, respectively. Furthermore, according to Fig. 8 and Eq. (5), the average mixing index for$L = \frac{\pi}{6}R_b$, $\frac{\pi}{3}R_b$, and $\frac{\pi}{2}R_b$can be obtained 48.1%, 56.6%, and 61.1%, respectively. Mixing at $L = \frac{\pi}{3}R_b$ is about 17.6% better than mixing at $L = \frac{\pi}{6}R_b$ and the average mixing index of $L = \frac{\pi}{2}R_b$ is 7.9% greater than that of $L = \frac{\pi}{3}R_b$. The positive effect of increased length on mixing performance can be explained as follows:
The blades with longer length promote unsteady boundary conditions, and thus the fluid elements will stretch and fold more rapidly, increasing chaos degree. In addition, the more volume of fluid is driven by blades as the blades with higher length are adopted, and therefore the regular and non-chaotic regions in the mixer are reduced. An important point that can be seen in both Figs. 5 and 7 is the horseshoe set with various sizes. The horseshoe set refers to a sample of stretched and folded tracer before dividing into two pieces. These horseshoes can be detected before the fluid surface is completely covered by the tracer. The formation of horseshoe sets in a mixer is one of the chaotic advection characteristics which has been also addressed by Chien et al. [3] for chaotic cavity flows. Also, a comparison between Figs. 6 and 8 shows that the influence of average rotational speed on mixing enhancement is more pronounced than that of the length of blades; in fact the average mixing index increases 146% as the average rotational speed increases from 7.5 to 30 rpm, while increasing the length of blades from $\frac{\pi}{6}R_b$ to $\frac{\pi}{2}R_b$ increases the average mixing index only about 27%. In other words, the folding and stretching phenomena are more affected by rotational velocity than blades length for the chaotic mixer under study.

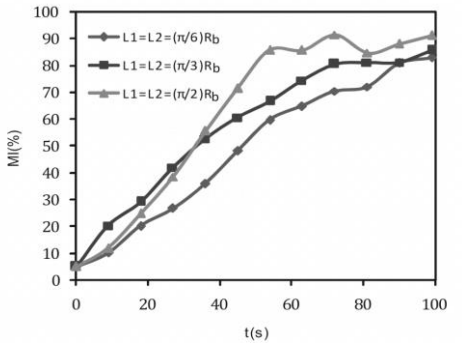

Fig. 8. Effect of the length of blades on mixing index ($\omega_{ave} = 15\ rpm$ and $\Delta\omega = 10\ rpm$ for all cases).

4.3. Effect of speed amplitude on mixing

As a stepwise motion protocol is used to rotate the rotational blades of mixer, the influence of rotational speed amplitude ($\Delta\omega = 5\ and\ 10\ rpm$) on mixing index is illustrated in Fig. 9.

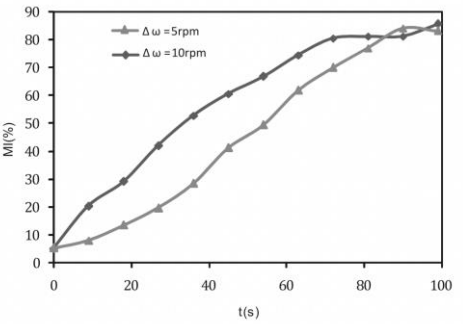

Fig. 9. Effect of rotational speed amplitude of blades on mixing index ($L = \frac{\pi}{3}R_b$ and $\omega_{ave} = 15\ rpm(Re \simeq 20)$ for both cases).

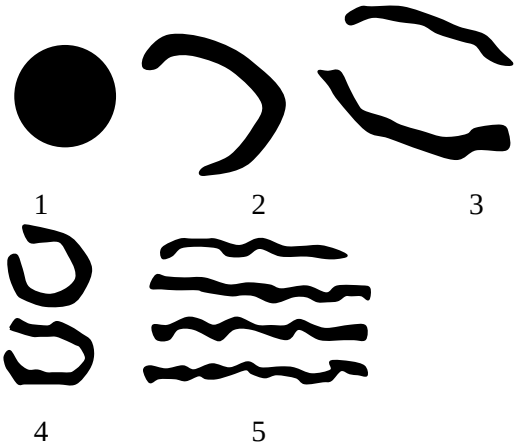

Fig. 10. Schematic of folding and stretching of blob tracer.

It is observed that the mixing index of $\Delta\omega = 10\ rpm$ is greater than that of $\Delta\omega = 5\ rpm$ until both mixing index profiles reach a steady state situation (at about t=81 s) when almost 90% of the free surface is covered by the dye. Furthermore, one can clearly see that the mixing time decreases with the increase of rotational speed amplitude, and required times to reach complete mixing for $\Delta\omega = 5\ and\ 10\ rpm$ cases are 90 s and 72 s, respectively. According to Fig. 9 and using Eq. (2), the average mixing index for $\Delta\omega = 5\ and\ 10\ rpm$ are obtained 45.1% and 56.6%, respectively. The reason of mixing enhancement in higher amplitude is due to a better condition of flow kinematic. Such flow kinematic can be attributed to the unsteady boundary conditions and acceleration of fluid particles which lead to a time-dependent perturbation in the mixer. Under this situation, fluid particles experience more area of the chaotic region with higher severity and consequently, folding and stretching of fluid elements occurs more rapidly compared to the situation in which the velocity variation of high-viscous fluid is not considerable. Therefore, the negative impact of low diffusivity of tracer into the base fluid is compensated by an increased interface which is a direct result of the successive folding and stretching phenomena occurring in the chaotic mixer. This point was also addressed in previous studies [6, 7, 16, 23-25]. In order to have a better understanding of the effect of the phenomena on mixing, the mechanism of blob tracer folding and stretching is schematically shown in Fig. 10. A tracer element is considered in an initial situation which has a low interface with the base fluid. As evident from this figure, due to successive folding and stretching phenomena, number pieces of tracer can be formed in the mixer and thus the interface between tracer and base fluid increases, causing a better condition for laminar mixing of high-viscous fluids.

4.4. Repeatability of experiments

The repeatability of the tests is one of the main points considered in experimental studies, but the most important feature of a chaotic system is sensitivity to initial conditions [25]. The question arises whether the obtained results in this study can be repeated in a similar experiment. In simple words, is the validity of the obtained results restricted to only this study? To answer this question, it can be stated that although the obtained results in two chaotic mixing tests with the same conditions cannot be exactly similar, the trend of mixing index is identical and the average values are close to each other. A similar discussion was explained by Mashaei [25] for a chaotic continues mixer applied in bread dough formation process in which the maximum error between data obtained by two similar chaotic systems was reported about 12%. Also, it was observed that the error in average mixing index between two similar tests does not exceed 4%. In order to evaluate the repeatability of the experiments, mixing index profiles related to $L = \frac{\pi}{3}R_b$ and $\omega_{ave} = 15$ case for two separate experiments are illustrated in Fig. 11. As evident from this figure, there is a good agreement between the results obtained by two similar, but separate experiments and the maximum local error is about 9%. Further, the average mixing indexes for two different tests are calculated at 48.89% and 46.53%, respectively, which indicates an error of less than 5%.

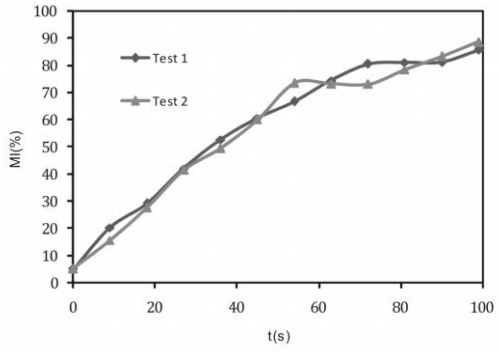

Fig. 11. Repeatability of experiments ($L = \frac{\pi}{3}R_b$, $\omega_{ave} = 15 (Re \simeq 20)$ and $\Delta\omega = 10\ rpm$ for both tests).

5. Conclusions

In this study, a novel approach to the design and manufacturing of a chaotic liquid mixer by applying two rotational blades with stepwise

motion in a circular vessel is introduced. The influence of various parameters such as average rotational speed of blades, the length of blades and rotational speed amplitude of blades on mixing performance is investigated by means of deformation of a material blob. Mixing performance is dramatically improved with increasing average blade rotational speed because of intensifying successive stretching and folding of fluid elements. It is demonstrated by experimental results that the increase in the length of blades can be considered as an essential factor leading to mixing improvement, preventing the formation of non-chaotic regions. A quantitative comparison shows that the role of average rotational speed of blades on mixing promotion is more pronounced than that of the length of blades. Furthermore, observations reveal that the agitation by an increased rotational speed amplitude leads to an effective mixing. The chaotic mixer suggested in this study may be applicable to a wide range of processes in which laminar mixing is required. Although the present study shows a high efficiency of the proposed mixer for laminar mixing of high-viscous flow, more numerical and experimental studies are needed to carry out to gain a better insight into mixing performance of this mixer. In addition, one of the most useful features of the novel chaotic mixer is to operate under low energy consumption. This fact is due to the blades shape that no normal stress is imposed on them from the high-viscous fluid. The experiments related to the measurement of the power consumption of the presented chaotic mixer under the various operating condition, and also the thermal performance of mixer as a chaotic heat exchanger for chemical and food applications are under study.

References

[1] H. Aref, "*Stirring* by chaotic advection", *Journal of Fluid Mechanic*, Vol. 143, pp. 1-21, (1984).

[2] H. Aref, and S. Balachandar, "Chaotic advection in a Stokes flow", *Physics of Fluids*, Vol. 29, No. 11, pp. 3515-3521, (1986).

[3] W. L. Chien, H. Rising, and J. M. Ottino, "Laminar mixing and chaotic mixing in several cavity flows", *Journal of Fluid. Mechanics*, Vol. 170, pp. 355-377, (1986).

[4] D. J. Lamberto, F. J. Muzzio, P. D. Swanson, and A. L. Tonkovich, "Using time-dependent RPM to enhance mixing in stirred vessels", *Chemical Engineering Science*, Vol. 51, No. 5, pp. 733-741, (1996).

[5] W. G. Yao, H. Sato, K. Takahashi, and K. Koyama, "Mixing performance experiments in impeller stirred tanks subjected to unsteady rotational speeds", *Chemical Engineering Science*, Vol. 53, No. 17, pp. 3031-3040, (1998).

[6] P. D. Swanson, and J. M. Ottino, "Comparative computational and experimental study of chaotic mixing of viscous fluids", *Journal of Fluid. Mechanics*., Vol. 213, pp. 227-227, (1990).

[7] H. Aref, and S. Balachandar, "Chaotic advection in a Stokes flow", Phys. Fluids., Vol. 29, No. 11, pp. 3515–3521, (1986).

[8] P. Dutta, and R. Chevray, "Effect of diffusion on chaotic advection in Stokes flow", *Physics of Fluids*, Vol. 3, No. 5, p.1440, (1991).

[9] J. A. Zambaux, J. L. Harion, S. Russeil, and P. Bouvier, "Combining two orthogonal secondary flows to enhance the mixing in an annular duct", *Chemical Engineering Research and Design*, Vol. 94, pp.702-713, (2012).

[10] O. S. Galaktionov, V. V. Meleshko, G. W. M. Peters, H. E. H., Meijer, "Stokes flow in a rectangular cavity with a cylinder", *Fluid. Dynamic Research*, Vol. 24, No. 2, pp. 81-102, (1999).

[11] K. Takahashi, and M. Motoda, "Chaotic mixing created by Object inserted in a vessel agitated by an impeller", *Chemical Engineering Research and Design*, Vol. 84, No. 4, pp. 386-390, (2009).

[12] Z. Zhang, and G. Chen, "Liquid mixing enhancement by chaotic perturbations in stirred tanks", *Chaos, Soliton and Fractal*, Vol. 36, No. 1, pp.144-149, (2008).

[13] Y. Kato, Y. Tada, M. Ban, Y. Nagatsu, S. Iwata, and K. Yanagimoto, "Improvement of Mixing Efficiencies of Conventional Impeller with Unsteady Speed in an Impeller Revolution", *Journal of Chemical Engineering of Japan*, Vol. 38, No. 9, pp. 688-691, (2005).

[14] K. Takahashi, H. Sekine, Y. Sugo, and Y. Takahata, "Nakamura M. Laminar Mixing in Stirred Tank Agitated by an Impeller Inclined", *International Journal of Chemical Engineering*, doi:10.1155/2012/858329 (2012).

[15] Y. Hwu, "Chaotic stirring in a new type of mixer with rotating rigid blades", *European Journal of Mechanic B-Fluid*, Vol. 27, No. 3, pp. 239-250, (2008).

[16] P. R. Mashaei, S. M. Hosseinalipour, M. J. Muslmani, N. M. Nouri, "Experimental study on chaotic mixing created by a new type of mixer with rotational blades", *Advances in Mechanical Engineering*, doi: 10.1155/2012/543253, (2012).

[17] M. Robinson, and W. Cleary, "Flow and mixing performance in helical ribbon mixers", *Chemical Engineering Science*, Vol. 84, pp. 382-398, (2012).

[18] Z. Liu, X. Zheng, D. Liu, Y. Wang, and C. Tao, "Enhancement of liquid–liquid mixing in a mixer-settler by a double rigid-flexible combination impeller", Chem. Eng. Process., Vol. 86, pp. 69-77, (2014).

[19] F. Shirmohammadi, A. Tohidi, "Mixing enhancement using chaos theory in fluid dynamics: Experimental and numerical study", *Chemical Engineering and Processing: Process Intensification*, In press, (2018).

[20] S. Y. Jung, K.H. Ahn, T. G. Kang, G. T. Park, S. U. Kim, "Chaotic Mixing in a Barrier-Embedded Partitioned Pipe Mixer", *AIChE Journal*, Vol. 64, No. 2, pp.717-729, (2018).

[21] S. Jegatheeswaran, F. Ein-Mozaffari, and W. Jiangning, "Efficient Mixing of Yield-Pseudoplastic Fluids at Low Reynolds Numbers in the Chaotic SMX Static Mixer, *Chemical Engineering Journal*, Vol. 317, pp.215-231, (2017).

[22] T. C. Niederkorn, and J. M. Ottino, "Mixing of a viscoelastic fluid in time-periodic flow", *Journal of Fluid Mechanic*, Vol. 256, pp. 243-268, (1993).

[23] S. M. Hosseinalipour, A. Tohidi, P. R. Mashaei, and A. S. Mujumdar, "Experimental investigation of mixing in a novel continuous chaotic mixer", *Koreaan Journal of Chemical Engineering*, Vol. 31, No. 10, pp. 1757-1765, (2014).

[24] Fox, Robert W. Alan, T. McDonald, and J. Philip Pritchard, Introduction to fluid mechanics (6th Ed.). Hoboken, NJ: Wiley (2006).

[25] P. R. Mashaei, Design and manufacturing of a chaotic mixer for non-Newtonian fluid, M.S. thesis, Iran University of Science and Technology, *Tehran*, Iran (2011).

How to cite this paper:

S. M. Hosseinalipour, P. R. Mashaei, M. E. J. Muslomani and M. Taheri, "Laminar mixing of high-viscous fluids by a novel chaotic mixer" *Journal of Computational and Applied Research in Mechanical Engineering*, Vol. 8, No. 2, pp. 199-210, (2018).

DOI: 10.22061/jcarme.2018.1681.1147

URL: http://jcarme.sru.ac.ir/?_action=showPDF&article=932